



HAL
open science

Torque observation of WRSM with model uncertainties for EV applications

Yahao Chen, Malek Ghanes, Arezki Fekik, Abdelmalek Maloum

► **To cite this version:**

Yahao Chen, Malek Ghanes, Arezki Fekik, Abdelmalek Maloum. Torque observation of WRSM with model uncertainties for EV applications. 2024. hal-04707882

HAL Id: hal-04707882

<https://hal.science/hal-04707882v1>

Preprint submitted on 24 Sep 2024

HAL is a multi-disciplinary open access archive for the deposit and dissemination of scientific research documents, whether they are published or not. The documents may come from teaching and research institutions in France or abroad, or from public or private research centers.

L'archive ouverte pluridisciplinaire **HAL**, est destinée au dépôt et à la diffusion de documents scientifiques de niveau recherche, publiés ou non, émanant des établissements d'enseignement et de recherche français ou étrangers, des laboratoires publics ou privés.



Distributed under a Creative Commons Attribution 4.0 International License

Torque observation of WRSM with model uncertainties for EV applications

Yahao Chen, Malek Ghanes *Member, IEEE*, Arezki Fekik and Abdelmalek Maloum

Abstract—In this paper, a torque observation method based on linear parameter varying (LPV) approach is proposed for a wound rotor synchronous machine (WRSM) used in Electric Vehicle (EV) car (mainly used in Renault ZOE car). The machine is modelled with the consideration of model uncertainties in both the magnetic behavior and the machine resistance. The uncertainties of the magnetic behavior come mainly from the saturation effect of the inductance and are viewed as extra state variables of the system. Then by treating the derivatives of the magnetic uncertainties as states and disturbance variables, the machine model in state space form is formulated as an LPV system or an equivalent nonlinear time-dependent system. State observability and unknown input observability are studied. Finally, a robust LPV observer is designed to estimate the flux and eventually the torque of the machine. Both simulation and experimental results are illustrated on a benchmark of EV propulsion to show the effectiveness of the proposed observer.

Index Terms—Wound rotor synchronous machine (WRSM), observability and observation, LPV observer, torque and flux estimation, uncertainties estimation, EV applications

I. INTRODUCTION

FOR safety and control reasons, the propulsion of electric vehicles (EVs/HEVs) is halted if the difference between the measured torque and the reference (accelerator pedal) exceeds a minimum threshold set by the manufacturers. Traditional torque measurement using mechanical sensors is costly and bulky. Therefore, torque information is often obtained through data prediction systems, which can limit accuracy. To improve torque estimation accuracy and reduce costs, software-based sensor methods that do not require mechanical sensors for permanent magnet synchronous machines (PMSMs) have been developed in e.g., [1], [2], [3]. A sensorless torque estimation method for brushless DC motors using back electromotive force (BEMF) and observer techniques to achieve accurate torque estimation is proposed in [4]. Similarly, another approach presents a sensorless torque estimation method for induction motors using a Luenberger observer [5]. This method is based on a mathematical model of the induction motor and allows for robust torque estimation despite varying operating conditions. The methods proposed in [1], [2], [3] take into account magnetic saturation and magnet demagnetization to ensure better torque estimation accuracy. These methods have been tested on a low-power test bench (1.5-3 kW) with a PMSM, and the

results were satisfactory. Indeed, the difference between the estimated torque and the requested torque (accelerator pedal) is below the set minimum threshold. However, when these methods were tested on the full-power test bench BEMEVE (<https://renault-chair.ec-nantes.fr/bemeve>), with a wound rotor synchronous motor (similar to those used in early generations of the ZOE EV), the torque estimator did not show sufficient robustness to variations of magnetic uncertainties [6]. Additionally, variations in stator resistance and speed were not considered.

In this paper, we propose a new torque observer that takes into account variations in magnetic uncertainties. The proposed LPV observer is distinguished by its ability to handle variations in magnetic uncertainties, stator resistances, and motor speed, thereby improving the accuracy and robustness of torque estimation. The originality of our approach lies in its consideration of a wide range of uncertainties and parameter variations, enabling more precise and robust torque estimation, essential for demanding EV applications. A rigorous observation methodology, including observability study, observer design, and stability analysis, is proposed. This approach is supported by experimental tests on a real-power test bench BEMEVE.

For the theoretical contributions, we first showcase the state and unknown-input observability of our machine WRSM by its nonlinear time-varying control system model. Subsequently, we propose a robust observer based on a linear parameter-varying (LPV) formulation. Over the past decades, the control and observation of LPV systems have been extensively studied both theoretically and in practical applications, as detailed in the survey by Hoffmann and Werner [7]. Notably, several works have demonstrated the effectiveness of LPV system formulations for EV applications, including [8]–[12]. Our approach differentiates itself by employing a torque observer with a Kalman-like structure [13] and utilizing polytopic synthesis [14]. Consequently, the gain scheduling is achieved through a finite number of quadratic matrix inequalities. We propose a straightforward algorithm that transforms these bilinear matrix inequalities (BMIs) into linear matrix inequalities (LMIs), which are then solved iteratively.

The remainder of the article is structured as follows: Section II presents the mathematical model of the WRSM. Section III describes the state and unknown input observability. Section IV details the robust LPV state observer design. Section V provides the simulation results. The experimental results and discussion, demonstrating the accuracy and robustness of the proposed method, are presented in Section VI. Finally, Section VII concludes the article and outlines future research perspectives.

Yahao Chen is with HYCOMES Team, Inria Center at Rennes University, France (e-mail: yahao.chen@inria.fr).

Malek Ghanes and Arezki Fekik are with Nantes University, Centrale Nantes, LS2N UMR CNRS 6004, France (e-mail: malek.ghanes@ls2n.fr, arezki.fekik@ls2n.fr).

Abdelmalek Maloum is with Ampere, Renault, TCR, Guyancourt, France (e-mail: abdelmalek.maloum@ampere.cars).

Remark 1. Generally, the model uncertainties arising from variations in resistance, ΔR_s and ΔR_r , can be viewed as slow-varying parameters in the system matrix or as external disturbances. However, here we do not regard them as varying parameters like ω_e . This exclusion stems from the challenge of accurately determining the bounds of these variations, which are necessary for robust LPV observer design. While both ΔR_s and ΔR_r are bounded, determining their values or bounds precisely is difficult. There are two reasons why these uncertainties are not treated as external disturbances d . Firstly, an examination of ΔA and B reveals that the resistance uncertainties and the known inputs u affect the system in similar directions. In cases where input voltages are sufficiently large, they can compensate for any adverse effects caused by ΔR_s and ΔR_r . Secondly, the primary objective of the LPV observer design below is to bolster robust performance against magnetic uncertainties rather than resistance uncertainties.

In practical systems, the angular velocity of the machine operates within a limited range due to physical constraints. Therefore, it is reasonable to assume that the parameter ω_e is bounded, meaning it falls within a specified range, i.e.,

$$\omega_e \in [\underline{\omega}_e, \bar{\omega}_e],$$

where $\bar{\omega}_e = \max(\omega_e)$ and $\underline{\omega}_e = \min(\omega_e)$ are constants. System (6) is called a *polytopic* LPV system [7], [18] because the system matrix A depends affinely on the varying parameter ω_e , i.e.,

$$A(\omega_e) \in \text{Co}\{A(\underline{\omega}_e), A(\bar{\omega}_e)\},$$

where $\text{Co}\{\cdot\}$ denotes a convex hull of matrices. More specifically, we can write

$$A(\omega_e) = \alpha(\omega_e)A(\underline{\omega}_e) + (1 - \alpha(\omega_e))A(\bar{\omega}_e),$$

where

$$0 \leq \alpha(\omega_e) = \frac{\bar{\omega}_e - \omega_e}{\bar{\omega}_e - \underline{\omega}_e} \leq 1. \quad (7)$$

Apart from the angular velocity, due to the physical operation limits and the reasons that the currents of the machine has already been regulated via a PI controller, we make the following boundness assumptions on the variables x , the resistance uncertainties ΔR_s , ΔR_f (or, equivalently, ΔA) and the acceleration $\dot{\omega}_e$.

Assumption 1. There exist positive scalars l_1, l_2, τ such that

$$\|\Delta A\| < l_1, \quad \|x\| < l_2, \quad \|\dot{\omega}_e\| < \tau.$$

If the angular velocity ω_e is viewed as a known input variable, then system (6) can be seen as a nonlinear system

$$\Sigma: \begin{cases} \dot{x} = f(x, \omega_e, \Delta R_s, \Delta R_f) + Bu + Ed \\ y = h(x), \end{cases} \quad (8)$$

where $f(x, \omega_e, \Delta R_s, \Delta R_f) = (A(\omega_e) + \Delta A)x$, $h(x) = Cx$. This nonlinear system model will be used for checking the state and unknown inputs/disturbance observability. Then a robust LPV observer will be built on system (6).

III. STATE AND UNKNOWN INPUT OBSERVABILITY

We adopt the classical definition of state observability for nonlinear systems in e.g., [19], [20]. Denote a solution of Σ starting from an initial point x^0 under some ω_e, u, d by $x(t, x^0; \omega_e, u, d)$.

Definition 1 (State observability). The system Σ is called locally state observable if there exists an open dense subset $V \subseteq \mathbb{R}^n$ and a time scalar $T > 0$ such that for any two states $x^1 \in V$ and $x^2 \in V$, the corresponding outputs with x^1 and x^2 as initial points satisfies that $y(t, x^1; \omega_e, u, d) \neq y(t, x^2; \omega_e, u, d)$ implies $x(t, x^1; \omega_e, u, d) \neq x(t, x^2; \omega_e, u, d)$ for all $t \in [0, T)$ and for all admissible u, d, ω_e .

Roughly speaking, the state observability is a property for the reconstruction of the state variables x via the data from the measurable outputs y and its time derivatives \dot{y}, \ddot{y}, \dots when assuming the inputs ω_e, u and d (and their time derivatives) are known. However, the disturbance d , a priori, is not given, to know if it is possible to use the available information y to recover d , we need to check its unknown input observability, the latter concept is closely related to the left-invertibility of nonlinear control systems [20]–[22].

Definition 2 (Left-invertibility and unknown input observability). The system Σ is called locally left-invertible with respect to inputs d and outputs y if there exists an open dense subset $V \subseteq \mathbb{R}^n$ and a time scalar $T > 0$ such that for any initial point $x^0 \in V$ and two admissible inputs $d^1(t)$ and $d^2(t)$, the corresponding outputs with d^1 and d^2 as inputs satisfies that $y(t, x^0; \omega_e, u, d^1) \neq y(t, x^0; \omega_e, u, d^2)$ implies $d^1(t) \neq d^2(t)$ for all $t \in [0, T)$ and for all admissible u, ω_e . The system Σ is called locally unknown input observable for d if it is locally left-invertible without knowing the initial value x^0 .

The input-observability characterizes the property of recovering the unknown inputs d by $y, \dot{y}, \ddot{y}, \dots$ (possibly need the help of u, ω_e and their derivatives) without the knowledge of x^0 . The criteria for checking the state or unknown input observability relies on the calculation of the time derivative array for the outputs y . Denote $L_f h(x, \omega_e) := \frac{\partial h(x, \omega_e)}{\partial x} f(x, \omega_e)$. For system Σ , given by (8), we have

$$\dot{y} = L_f h(x, \omega_e) + L_B h \cdot u + L_E h \cdot d,$$

where

$$L_f h(x, \omega_e) = C(A(\omega_e) + \Delta A)x, \quad L_B h = CB, \quad L_E h = 0.$$

Then

$$\begin{aligned} \ddot{y} &= L_f^2 h(x, \omega_e) + \frac{\partial L_f h}{\partial \omega_e}(x) \dot{\omega}_e + L_B L_f h(\omega_e) \cdot u \\ &\quad + L_E L_f h \cdot d + L_B h \cdot \dot{u} + L_E h \cdot \dot{d}, \end{aligned}$$

where

$$L_f^2 h(x, \omega_e) = C(A(\omega_e) + \Delta A)^2 x, \quad \frac{\partial L_f h}{\partial \omega_e}(x) = C \frac{\partial A(\omega_e)}{\partial \omega_e} x,$$

$$\begin{aligned} L_B L_f h(\omega_e) &= C(A(\omega_e) + \Delta A)B, \\ L_E L_f h &= C(A(\omega_e) + \Delta A)E. \end{aligned}$$

It can be seen that the Jacobian matrix

$$O(\omega_e, \dot{\omega}_e) = \frac{\partial(y, \dot{y}, \ddot{y})}{\partial x} = \begin{bmatrix} C \\ C(A(\omega_e) + \Delta A) \\ C(A(\omega_e) + \Delta A)^2 + C \frac{\partial A(\omega_e)}{\partial \omega_e} \dot{\omega}_e \end{bmatrix} = \begin{bmatrix} 1 & 0 & 0 & 0 & 0 & 0 & 0 & 0 \\ 0 & 1 & 0 & 0 & 0 & 0 & 0 & 0 \\ 0 & 0 & 1 & 0 & 0 & 0 & 0 & 0 \\ \frac{\tilde{R}_s L_f}{L_\delta} & \frac{-L_f L_q \omega_e}{L_\delta} & \frac{-\tilde{R}_f M_f}{L_\delta} & 0 & \frac{-L_f \omega_e}{L_\delta} & \frac{L_f}{L_\delta} & 0 & \frac{-M_f}{L_\delta} \\ \frac{-\omega_e L_d}{L_q} & \frac{-\tilde{R}_s}{L_q} & \frac{-\omega_e M_f}{L_q} & \frac{-\omega_e}{L_q} & 0 & 0 & \frac{-1}{L_q} & 0 \\ \frac{-\tilde{R}_s M_f}{L_\delta} & \frac{M_f L_q \omega_e}{L_\delta} & \frac{\tilde{R}_f L_d}{L_\delta} & 0 & \frac{M_f \omega_e}{L_\delta} & \frac{-M_f}{L_\delta} & 0 & \frac{L_d}{L_\delta} \\ * & * & * & A_{74} & A_{75} & A_{76} & A_{77} & A_{78} \\ * & * & * & A_{84} & A_{85} & A_{86} & A_{87} & A_{88} \\ * & * & * & A_{94} & A_{95} & A_{96} & A_{97} & A_{98} \end{bmatrix},$$

where $\tilde{R}_s = R_s + \Delta R_s$, $\tilde{R}_f = R_f + \Delta R_f$, $A_{74} = \frac{L_f}{L_\delta} \omega_e^2$, $A_{75} = -\frac{L_f^2 \tilde{R}_s}{L_\delta^2} \omega_e - \frac{\tilde{R}_f M_f^2}{L_\delta^2} \omega_e - \frac{L_f}{L_\delta} \dot{\omega}_e$, $A_{76} = \frac{\tilde{R}_s L_f^2}{L_\delta^2} + \frac{\tilde{R}_f M_f^2}{L_\delta^2} - \frac{L_f}{L_\delta} \omega_e$, $A_{77} = 0$, $A_{78} = -\frac{\tilde{R}_s L_f M_f}{L_\delta^2} - \frac{\tilde{R}_f M_f L_d}{L_\delta^2}$, $A_{84} = \frac{\tilde{R}_s}{L_q} \omega_e - \frac{1}{L_q} \dot{\omega}_e$, $A_{85} = -\frac{1}{L_q} \omega_e^2$, $A_{86} = 0$, $A_{87} = \frac{\tilde{R}_s}{L_q^2}$, $A_{88} = 0$, $A_{94} = -\frac{M_f}{L_\delta} \omega_e^2$, $A_{95} = \frac{\tilde{R}_s M_f L_f}{L_\delta^2} \omega_e + \frac{\tilde{R}_f M_f L_d}{L_\delta^2} \omega_e + \frac{M_f}{L_\delta} \dot{\omega}_e$, $A_{96} = -\frac{\tilde{R}_s M_f L_f}{L_\delta^2} - \frac{\tilde{R}_f L_d M_f}{L_\delta^2} + \frac{M_f}{L_\delta} \omega_e$, $A_{97} = 0$, $A_{98} = \frac{\tilde{R}_s M_f^2}{L_\delta^2} + \frac{\tilde{R}_f L_d^2}{L_\delta^2}$ and the symbol “*” represents irrelevant terms. The following results concern with the state and unknown input observability of the system.

Theorem 1. *The system Σ , given by (8), is state observable for all $x \in \mathbb{R}^n$ if and only if*

$$|\dot{\omega}_e| \neq \omega_e^2. \quad (9)$$

Moreover, Σ is left-invertible with respect to the unknown input d but it is not unknown input observable.

Proof. We can find two matrix-valued functions $P(\omega_e) \in \mathbb{R}^{9 \times 9}$ and $Q(\omega_e) \in \mathbb{R}^{8 \times 8}$, which are invertible for all $\omega_e \in \mathbb{R}$, such that

$$\tilde{O}(\omega_e, \dot{\omega}_e) = P(\omega_e) O(\omega_e, \dot{\omega}_e) Q(\omega_e) = \begin{bmatrix} 1 & 0 & 0 & 0 & 0 & 0 & 0 & 0 \\ 0 & 1 & 0 & 0 & 0 & 0 & 0 & 0 \\ 0 & 0 & 1 & 0 & 0 & 0 & 0 & 0 \\ 0 & 0 & 0 & 0 & 0 & \frac{L_f}{L_\delta} & 0 & \frac{-M_f}{L_\delta} \\ 0 & 0 & 0 & 0 & 0 & 0 & \frac{-1}{L_q} & 0 \\ 0 & 0 & 0 & 0 & 0 & \frac{-M_f}{L_\delta} & 0 & \frac{L_d}{L_\delta} \\ 0 & 0 & 0 & \omega_e^2 & \dot{\omega}_e & 0 & 0 & 0 \\ 0 & 0 & 0 & \dot{\omega}_e & \omega_e^2 & 0 & 0 & 0 \\ 0 & 0 & 0 & 0 & 0 & 0 & 0 & 0 \end{bmatrix}.$$

Recall from Corollary 4.11 of [20] that the system Σ is state-observable if and only if $\text{rank } O(\omega_e, \dot{\omega}_e) = 8$. The matrix \tilde{O} (and thus O) is of rank 8 if and only if the matrix $\begin{bmatrix} \omega_e^2 & \dot{\omega}_e \\ \dot{\omega}_e & \omega_e^2 \end{bmatrix}$ is non-singular. The latter condition is equivalent to (9). Hence Σ is state observable if and only if (9) holds.

Moreover, it can be seen from the calculations of \dot{y} and \ddot{y} that the vector relative degree [20], [23] of Σ with respect to y and d is (2, 2) since $L_E h = 0$ and $L_E L_f h$ is invertible. So the system Σ is left-invertible with respect to y and d because $d = (L_E L_f h)^{-1} (\ddot{y} - L_f^2 h(x, \omega_e) - \frac{\partial L_f h}{\partial \omega_e}(x) \dot{\omega}_e - L_B L_f h(\omega_e) \cdot u - L_B h \cdot \dot{u})$. Thus given the same initial condition x^0 , any two different outputs $y^1(t, x^0; \omega_e, u, d^1) \neq y^2(t, x^0; \omega_e, u, d^2)$ must imply $d^1(t) \neq d^2(t)$. However, since it is not possible to express x (and thus x^0 and d) as some functions of $y, \dot{y}, u, \dot{u}, \omega, \dot{\omega}$ if x^0 is unknown, we have that $y^1(t, x^0; \omega_e, u, d^1) \neq$

$y^2(t, \hat{x}^0; \omega_e, u, d^2)$ does not necessarily imply $d^1(t) \neq d^2(t)$. Therefore, Σ is not unknown input observable for d . \square

Remark 2. (i) The ranks of $O(\omega_e, \dot{\omega}_e)$ and $L_E L_f h$, and thus the state observability and unknown input observability of Σ , are not determined by the resistance uncertainties ΔR_s and ΔR_f . However, in order to *exactly* estimate $x(t)$ or $d(t)$ using $x^0, y(t), u(t), \omega_e(t)$ and their derivatives, the precise values of the resistances are necessary. Although the latter data is not available, we can still design an observer to estimate the state $x(t)$ with bounded errors if ΔR_s and ΔR_f are assumed to be bounded.

(ii) Since $d(t)$ are not observable via the outputs y , we will treat them as unknown disturbances, to minimum its side effect to a state observer, the robustness of the observer against external disturbances should be addressed during design process.

IV. ROBUST LPV STATE OBSERVER

A. Observer design

Now for the polytopic LPV system $\Sigma(\omega_e)$, we seek a Kalman-like LPV observer in the form

$$\hat{\Sigma}(\omega_e) : \begin{cases} \dot{\hat{x}} = A(\omega_e) \hat{x} + B u + K(\omega_e)(y - C \hat{x}) \\ \hat{y} = \hat{C} \hat{x}, \end{cases} \quad (10)$$

where $\hat{x} = (\hat{i}_d, \hat{i}_q, \hat{i}_f, \hat{g}_d, \hat{g}_q, \hat{c}_d, \hat{c}_q, \hat{c}_f) \in \mathbb{R}^8$ are the states of the observer, $K(\omega_e) \in \mathbb{R}^{8 \times 3}$ is the observer gain which will be designed below and

$$\hat{C} = \begin{bmatrix} 0 & 0 & 0 & 1 & 0 & 0 & 0 & 0 \\ 0 & 0 & 0 & 0 & 1 & 0 & 0 & 0 \end{bmatrix},$$

which is defined for the robust performance on the estimations of g_d and g_q . Define the error e as the difference between the real states x and the estimated ones \hat{x} ,

$$e := x - \hat{x}.$$

Then the dynamics of the error and the performance outputs $y_e := \hat{C} x - \hat{y}$ are given by

$$\begin{cases} \dot{e} = (A(\omega_e) - K(\omega_e)C)e + E d + \Delta A x \\ y_e = \hat{C} e. \end{cases}$$

In order to minimize the effect of the disturbance for the estimation, our objective to design a robust LPV observer defined below.

Definition 3. The observer $\hat{\Sigma}(\omega_e)$ is called a robust LPV H_∞ observer for system $\Sigma(\omega_e)$ with performance $\gamma > 0$ if

- (i) $e(t) \rightarrow 0$ as $t \rightarrow \infty$ when $d = 0$ and $\Delta R_s = \Delta R_f = 0$.
- (ii) $\sup_{\omega_e \in [\underline{\omega}_e, \bar{\omega}_e]} \sup_{\|d\| \neq 0} \frac{\|y_e\|_2}{\|d\|_2} \leq \gamma$.

The following theorem states sufficient conditions for the existence of a robust LPV H_∞ observers for system $\Sigma(\omega_e)$.

Theorem 2. Under Assumption 1, there exists a robust LPV H_∞ observer $\hat{\Sigma}(\omega_e)$ for system $\Sigma(\omega_e)$ if there exist a matrix-valued function $P(\omega_e) = P^T(\omega_e) > 0$ and a positive scalar $\gamma > 0$ such that $\forall \omega_e \in [\underline{\omega}_e, \bar{\omega}_e]$:

$$\begin{bmatrix} S(\omega_e) & P(\omega_e) & P(\omega_e)E & \hat{C}^T \\ P(\omega_e) & -Q^{-1} & 0 & 0 \\ E^T P(\omega_e) & 0 & -\gamma I & 0 \\ \hat{C} & 0 & 0 & -\gamma I \end{bmatrix} < 0, \quad (11)$$

where

$$S(\omega_e) = A(\omega_e)^T P(\omega_e) + P(\omega_e)A(\omega_e) - C^T R^{-1} C \pm \tau \frac{\partial P(\omega_e)}{\partial \omega_e},$$

and $Q = Q^T > 0$, $R = R^T > 0$ are constant weighing matrices to tune. The observer gain is given by $K(\omega_e) = P^{-1}(\omega_e)C^T R^{-1}$. Moreover, if the resistances uncertainties ΔR_s and ΔR_f are not zero but bounded, then the errors $e(t)$ are also bounded.

Proof. Consider a Lyapunov function candidate:

$$V(e, t) = e^T P(\omega_e(t))e.$$

It follows that

$$\begin{aligned} \frac{dV(e, t)}{dt} &= \dot{e}^T P(\omega_e)e + e^T \dot{P}(\omega_e)e + e^T P(\omega_e)\dot{e} \\ &= e^T (A^T(\omega_e)P(\omega_e) - C^T R^{-1}C)e + d^T E^T P(\omega_e)e + \\ & x^T (\Delta A)^T e + e^T \dot{\omega}_e \frac{\partial P(\omega_e)}{\partial \omega_e} e + e^T P(\omega_e)Ed + \\ & e^T \Delta Ax + e^T (P(\omega_e)A(\omega_e) - C^T R^{-1}C)e \\ &= e^T (A^T(\omega_e)P(\omega_e) + P(\omega_e)A(\omega_e) - C^T R^{-1}C)e + \\ & \dot{\omega}_e e^T \left(\frac{\partial P(\omega_e)}{\partial \omega_e} \right) e + d^T E^T P(\omega_e)e + e^T P(\omega_e)Ed + \\ & x^T (\Delta A)^T e + e^T \Delta Ax - e^T C^T R^{-1}Ce. \end{aligned}$$

Now if (11) holds, then, by Schur complement, we have

$$\begin{bmatrix} S(\omega_e) + P(\omega_e)QP(\omega_e) & P(\omega_e)E \\ E^T P(\omega_e) & -\gamma^2 I \end{bmatrix} + \begin{bmatrix} \hat{C}^T \\ 0 \end{bmatrix} \begin{bmatrix} \hat{C} & 0 \end{bmatrix} < 0$$

That means

$$e^T (S(\omega_e) + P(\omega_e)QP(\omega_e))e + d^T E^T P(\omega_e)e + d^T P(\omega_e)Ee + y_e^T y_e - \gamma^2 d^T d < 0.$$

As a consequence, we have

$$\begin{aligned} f(\omega_e, \dot{\omega}_e) &:= \\ & e^T (A^T(\omega_e)P(\omega_e) + P(\omega_e)A(\omega_e) - C^T R^{-1}C)e + \\ & e^T \left(P(\omega_e)QP(\omega_e) + \dot{\omega}_e \frac{\partial P(\omega_e)}{\partial \omega_e} \right) e + d^T E^T P(\omega_e)e + \\ & e^T P(\omega_e)Ed + y_e^T y_e - \gamma^2 d^T d < 0. \end{aligned} \quad (12)$$

It follows that

$$\begin{aligned} \frac{dV(e, t)}{dt} + y_e^T y_e - \gamma^2 d^T d + e^T P(\omega_e)QP(\omega_e)e + \\ e^T C^T R^{-1}Ce - x^T (\Delta A)^T e - e^T \Delta Ax = f(\omega_e, \dot{\omega}_e) < 0. \end{aligned} \quad (13)$$

If $\Delta R_s = \Delta R_f = 0$, then $\Delta A = 0$ and thus

$$\begin{aligned} \frac{dV(e, t)}{dt} + y_e^T y_e - \gamma^2 d^T d < -e^T P(\omega_e)QP(\omega_e)e \\ - e^T C^T R^{-1}Ce < 0. \end{aligned}$$

Then it follows by classical robust control theory [24] that conditions (i) and (ii) of Definition 3 are satisfied, so $\hat{\Sigma}(\omega_e)$ is a robust LPV observer. Moreover, consider the case that ΔR_s and ΔR_f are nonzero. Recall from Assumption 1 that $\|\Delta A\| < l_1$ and $\|x\| < l_2$. Since $P(\omega_e)QP(\omega_e) + C^T R^{-1}C > 0$, there exists $\lambda > 0$ such that $\|P(\omega_e)QP(\omega_e) + C^T R^{-1}C\| > \lambda$. Then by (13) with $d = 0$, we have

$$\frac{dV(e, t)}{dt} < -\lambda \|e\|^2 + l_1 l_2 \|e\|.$$

Thus $e(t)$ remains bounded as for $\|e(t)\| > \frac{l_1 l_2}{\lambda}$, we have $\frac{dV(e, t)}{dt} < 0$. \square

B. Polytopic LPV synthesis

In order use the above results to find an observer gain $K(\omega_e)$, we need to render the infinite set of LMIs in (11) to a finite set of LMIs (or BMIs). There are different approaches for LPV synthesis as shown in the survey [7] and the references therein. Since our LPV system $\Sigma(\omega_e)$ is polytopic and only the system matrix A depends on ω_e , we will use the *polytopic synthesis* [14], [18]. Denote

$$A_1 = A(\underline{\omega}_e) \text{ and } A_2 = A(\bar{\omega}_e).$$

Corollary 1. Under Assumption 1, there exists a robust LPV H_∞ observer if there exist two positive-definite constant matrices $P_1 = P_1^T > 0$, $P_2 = P_2^T > 0$ and a positive scalar $\gamma > 0$ such that $\forall i, j = 1, 2$:

$$\begin{bmatrix} A_i^T P_i + P_i A_i - C^T R^{-1} C + \tilde{\tau}(P_i - P_j) & P_i & P_i E & \hat{C}^T \\ P_i & -Q^{-1} & 0 & 0 \\ E^T P_i & 0 & -\gamma I & 0 \\ \hat{C} & 0 & 0 & -\gamma I \end{bmatrix} < 0, \quad (14a)$$

$$(A_1 - A_2)^T (P_1 - P_2) + (P_1 - P_2)(A_1 - A_2) + (P_1 - P_2)Q(P_1 - P_2) \geq 0, \quad (14b)$$

where $\tilde{\tau} = \frac{\tau}{\bar{\omega}_e - \underline{\omega}_e}$, $Q = Q^T > 0$ and $R = R^T > 0$ are tuning matrices. The observer gain $K(\omega_e) = P^{-1}(\omega_e)C^T R^{-1}$, where $P(\omega_e) = \alpha(\omega_e)P_1 + (1 - \alpha(\omega_e))P_2$ and α is given by (7).

Proof. Observe that $f(\omega_e, \dot{\omega}_e)$ of (12) is a quadratic function of ω_e . By Lemma 3.1 of [14], $\forall \omega_e \in [\underline{\omega}_e, \bar{\omega}_e]$ and $\forall |\dot{\omega}_e| < \tilde{\tau}(\bar{\omega}_e - \underline{\omega}_e)$: $f(\omega_e) < 0$ if

$$\frac{\partial^2 f(\omega_e, \dot{\omega}_e)}{\partial \omega_e^2} = \left(\frac{\partial \alpha(\omega_e)}{\partial \omega_e} \right)^2 \frac{\partial^2 f}{\partial \alpha^2} \geq 0, \quad (15)$$

together with $\forall \omega_e \in \{\underline{\omega}_e, \bar{\omega}_e\}$ and $\forall \dot{\omega}_e \in \{-\tilde{\tau}(\bar{\omega}_e - \underline{\omega}_e), \tilde{\tau}(\bar{\omega}_e - \underline{\omega}_e)\}$:

$$f(\omega_e, \dot{\omega}_e) < 0. \quad (16)$$

Observe that

$$\begin{aligned} \frac{\partial^2 f}{\partial \alpha^2} = e^T ((A_1 - A_2)^T (P_1 - P_2) + (P_1 - P_2)(A_1 - A_2) + \\ (P_1 - P_2)Q(P_1 - P_2))e, \end{aligned}$$

thus (14b) implies (15). Moreover, by using Schur complement and $\frac{\partial P(\omega_e)}{\partial \omega_e} = \frac{1}{\bar{\omega}_e - \underline{\omega}_e}(P_1 - P_2)$, it is seen that (14a) guarantees (16) holds at the corners of the ranges for ω_e and $\dot{\omega}_e$. Therefore, with the same arguments in the proof of Theorem 2, we can conclude that $K(\omega_e) = P^{-1}(\omega_e)C^T R^{-1}$ with $P(\omega_e) = \alpha P_1 + (1 - \alpha)P_2$ is the observer gain for a robust LPV observer. \square

Note that the constraint (14b) is not an LMI but a BMI which depends quadratically on the unknowns and it is a *non-convex* optimization problem if one wants to minimize γ . It is *not* possible to transform simultaneously both (14a) and (14b) into LMIs by Schur complement or changing of variables. To solve this problem, one may use e.g. the methods in [25], [26]. Here we propose a simple solution with possible conservatism but easy for calculation and realization.

Step 1: Minimize $\gamma > 0$ under the LMIs constraints (14a) and

$$(A_1 - A_2)^T(P_1 - P_2) + (P_1 - P_2)(A_1 - A_2) + L_0 \geq 0, \quad L_0 > 0.$$

Denote the resulting P_1 and P_2 as P_{10} and P_{20} .

Step 2: If $L_0 \leq (P_{10} - P_{20})Q(P_{10} - P_{20})$, then stop and return to P_{10} and P_{20} . Otherwise, set $k = 1$ and go to Step 3.

Step 3: Minimize $\gamma > 0$ under the LMIs constraints (14a) and

$$(A_1 - A_2)^T(P_1 - P_2) + (P_1 - P_2)(A_1 - A_2) + L_k \geq 0, \\ L_{k-1} - L_k > 0.$$

Denote the resulting P_1 and P_2 as P_{1k} and P_{2k} .

Step 4: If $L_k \leq (P_{1k} - P_{2k})Q(P_{1k} - P_{2k})$, then stop and return to P_{1k} and P_{2k} . Otherwise, set $k = k + 1$ and go to Step 3.

Remark 3. (i) It is also possible to choose a Lyapunov function $V(e) = e^T P e$ that does not depend on ω_e . This choice simplifies the synthesis of the observer gain since the quadratic terms in (11) become affine-dependent on ω_e and $\frac{\partial P}{\partial \omega_e} = 0$. Consequently, the polytopic LPV synthesis method described in [18] can be applied, resulting in only two LMI constraints for $\omega_e = \underline{\omega}_e$ and $\omega_e = \bar{\omega}_e$. However, this method is more conservative compared to the one presented in Corollary 1 as the Lyapunov function is not parameter-dependent.

(ii) As our system has only one varying parameter ω_e , it is also convenient to apply the *girding-based* LPV synthesis [7], [27], [28]. The idea is to define a grid \mathcal{G} for $[\underline{\omega}_e, \bar{\omega}_e]$, then minimize γ under the LMIs defined by (11) with all $\omega_e \in \mathcal{G}$. Then check if the obtained P_1 and P_2 satisfy (11) under a denser grid. If it fails, increase the density of \mathcal{G} and resolve the LMIs. The girding-based method is easy to be implemented but such a method does not provide any rigorous guarantees for global convergence and performance [7].

C. Discussions and comparisons with existing results

Recall the results in [1] that a linear time-varying (LTV) observer was designed for the torque estimation of PMSMs, where the observer gain $K(t) = P^{-1}(t)C^T R^{-1}$ is calculated by solving the time-varying Riccati equation

$$\frac{dP(t)}{dt} = -A^T(t)P(t) - P(t)A(t) - P(t)QP(t) + C^T R^{-1}C, \quad (17)$$

where $A(t) = A(\omega_e(t))$ is viewed as a time-varying matrix by incorporating the online estimated value of ω_e . We now

Parameters	Value
Maximum Power	65 KW
Number of pole pairs (p)	2
Stator winding resistance (R_s)	0.0123 Ω
Stator's d -axis inductance (L_d)	$1700e^{-6}$ H
Stator's q -axis inductance (L_q)	$650e^{-6}$ H
Self inductance of field winding (L_f)	1.35 H
Mutual stator-rotor inductance (M_f)	0.0283H
Moment of inertia	$0.022Kg.m^2$
Coefficient of viscous friction	$0.0064Nm.s$

TABLE I
WRSM PARAMETERS OF THE FIRST ZOE CAR.

compare the LPV observer proposed in the present paper with the LTV observer in [1].

- The system model in [1] assumes that the magnetic uncertainties satisfy $\dot{g}_d = \dot{g}_q = 0$, limiting its observer to handling only slow-varying uncertainties. The proposed model Σ_e in (6) addresses magnetic uncertainties by treating \dot{g}_d and \dot{g}_q as state variables, with \ddot{g}_d and \ddot{g}_q considered as disturbances. This approach accommodates both slow and fast-varying uncertainties.
- A significant challenge in LTV observer synthesis is verifying the solvability of the time-varying Riccati equation (17). Even if $\Sigma(\omega_e(t))$ is observable at each point in time, this does not ensure the solvability of (17), which requires uniform complete observability [13]. In contrast, the existence of an LPV observer gain $P(\omega_e)$ can be pre-verified through the solvability of the LMIs (14a) and (14b).
- Another advantage of LPV observer synthesis is the computational cost. The LPV observer gain is calculated offline, whereas the LTV observer requires the online computation of $P(t)$ by solving (17), which is computationally intensive.

V. SIMULATION RESULTS

A WRSM with the parameters shown in Table I is simulated in the MATLAB/Simulink environment. The model is based on the formulation presented in (6), where the dynamics of the magnetic uncertainties g_d and g_q are taken into account. A standard PI field-oriented controller is applied to the machine. Simulations are conducted to verify the effectiveness of the proposed method under significant tests involving magnetic uncertainties ΔM_f and ΔL_d . The first test involves a 14% variation in M_f , while the second test examines a 5% variation in L_d .

These tests are realized with low speed (between 500 rpm and 600 rpm) of the WRSM under different torque commands. The results displayed in Figures 1 and 3, show the robustness of the proposed observer under the considered magnetic uncertainties, the torque is well estimated during the motor mode (torque command is increasing) and breaking mode decreasing (torque command is decreasing).

A. Results with magnetic uncertainties on mutual inductance

Figure 1 illustrates the reference torque T_{ref} along with the estimated torque T_{est} (LPV) using the LPV observer over

a span of 50 seconds. This analysis includes both static and dynamic variations in mutual inductance M_f . It is evident that the LPV observer performs excellently in tracking a piecewise constant torque reference, which is a common scenario in real-life driving conditions. Figure 2 presents a comparison between the LPV and LTV formulations during the initial 10 seconds. Notably, during the dynamic changes occurring between 3 and 6 seconds, the robust LPV observer precisely estimates the electromagnetic torque, whereas the LTV method encounters difficulties in correcting torque estimation errors, particularly at $t = 2$ seconds. This issue is likely due to challenges in solving the time-varying Riccati equation, highlighting the reliability of the LPV approach. Additionally, from 2 to 3 seconds, the LPV observer consistently outperforms the LTV method. The LPV method also demonstrates less overshoot compared to the LTV method when dealing with sudden changes, such as the step function at 6 seconds, in M_f . Overall, both techniques provide commendable estimates of electromagnetic torque throughout the testing period.

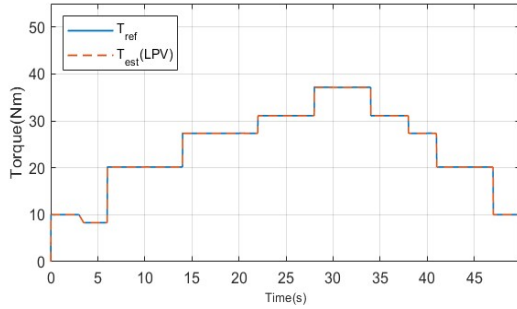


Fig. 1. Simulation results of LPV observer for 50s with variations on M_f .

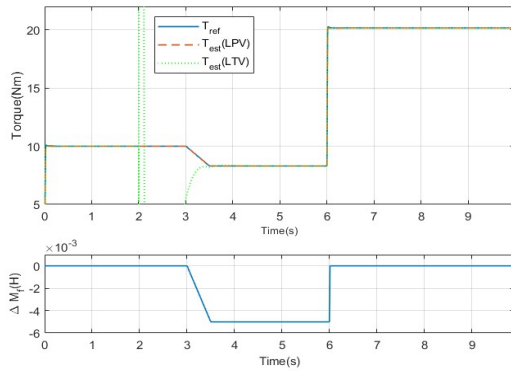


Fig. 2. Simulation results of LPV and LTV observers for 10s with variations on M_f .

B. Results with magnetic uncertainties on stator inductance

Figures 3 and 4 showcase the actual torque compared to the torque estimated by the LPV and LTV methods, with a focus

on variations in the stator's d -axis inductance L_d . This test is designed to highlight the effects of high-order derivatives of inductance variations. To simulate these effects, a sine function is used to modulate the d -axis inductance uncertainty. During the first phase of the simulation (from 0 to 4 seconds), the LTV observer displays significant oscillations. This occurs because the LTV observer's design does not account for the presence of high-order derivatives of uncertainties, and the sine function introduces non-trivial high-order time derivatives that contradict this assumption. In contrast, the LPV method shows robustness against such high-order derivatives, providing a relatively accurate torque estimation during this period. Furthermore, the LPV method benefits from a simpler structure and lower computational costs for gain calculation, resulting in faster tracking performance. After the initial phase, both methods deliver satisfactory torque estimations, demonstrating their effectiveness in capturing the system dynamics.

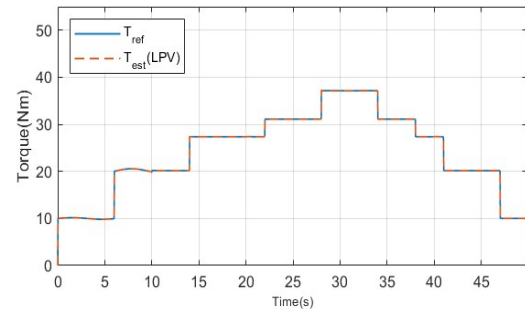


Fig. 3. Simulation results of LPV observer for 50s with uncertainties on L_d .

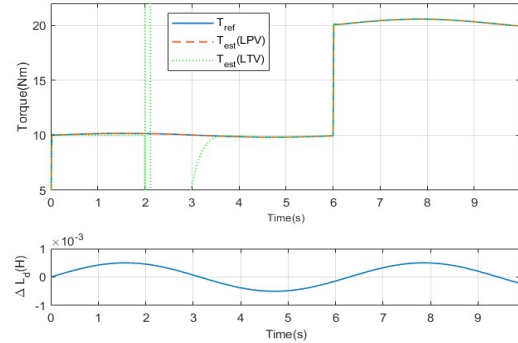


Fig. 4. Simulation results of LPV and LTV observers for 10s with uncertainties on L_d .

Remark 4 (Resistances uncertainties). The simulations with uncertainties in the resistances R_s and R_f have also been conducted. The estimation results show no significant differences when considering ΔR_s and ΔR_f to be zero or small values. The possible reasons for this have been explained in Remark 1 above. Specifically, the PI controller may compensate for the

side effects caused by ΔR_s and ΔR_f , and the torque T_e of (2) has no direct connections with the resistances.

VI. EXPERIMENTAL RESULTS

To assess the simulation results of the proposed observer based LPV approach, experiments tests are realized on the BEMEVE test bench (<https://renault-chair.ec-nantes.fr/bemeve>), which is dedicated to test EV motors at 1-scale power level.

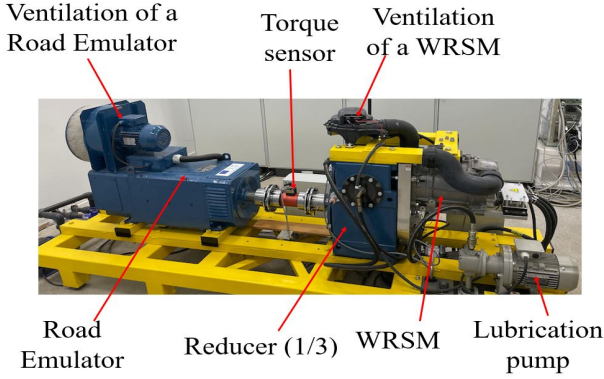


Fig. 5. BEMEVE test bench of electric motors for EVs

The tested motor is a WRSM, which is used in the first generation of ZOE cars with the same parameters used in simulation (Table I). A first test, which is the same one considered in simulation, is conducted at significant driving conditions. A second test is performed to show the interest of the uncertainties estimation of g_d and g_q for the torque observer.

A. Low speed (between 500 and 600 rpm) with different torque commands:

As in the simulation, this test corresponds to the driver’s demand when pressing the car’s acceleration pedal under a constant speed profile (road profile). The obtained results, shown in Figs. 6 and 7, are quite similar to those obtained in the simulation (Figs. 1 and 3). They reveal well-estimated torque when the torque command is increasing (motor mode) and decreasing (braking mode), despite the torque measurement being very noisy. We also notice the excellent performance of the torque estimation during dynamic phases of driving, such as rapid acceleration and deceleration. As expected, this performance is achieved by considering the higher-order time derivatives of the magnetic uncertainties g_d, g_q , which are managed by the proposed observer (9). The currents in the $d - q$ frame also perform well. As shown in Fig. 7, they are estimated with high precision, contributing to the accurate torque estimation.

B. Torque observer without uncertainties estimation:

To highlight the interest of the proposed observer, a test is conducted with constants speed and torque command. In this test, the estimated values of uncertainties g_d and g_q are not included in the torque estimation (Fig. 8) during intervals of time $[0, 4s]$ and $[10, 14s]$. As it can be seen, the torque

estimation, during these intervals of time, doesn’t performs well, a significant static error estimation appeared. Concerning the currents in $d - q$ frame, they are well estimated (Fig. 9) since they don’t depend on uncertainties estimation.

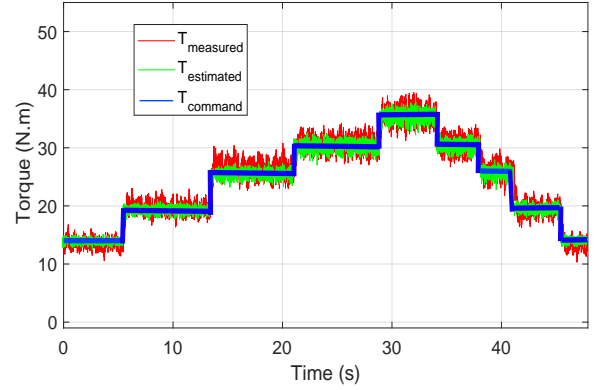


Fig. 6. Torque estimation results with the consideration of g_d, g_q .

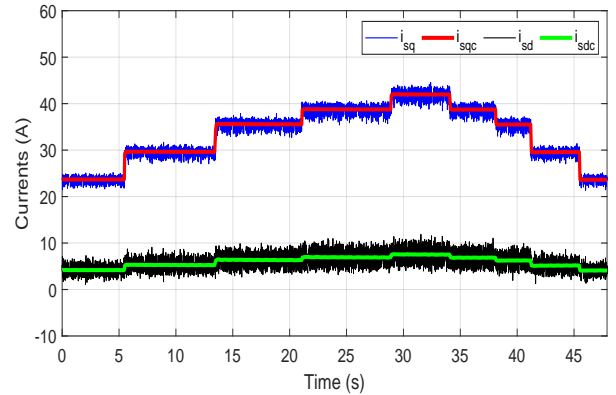


Fig. 7. The currents with the consideration of g_d, g_q .

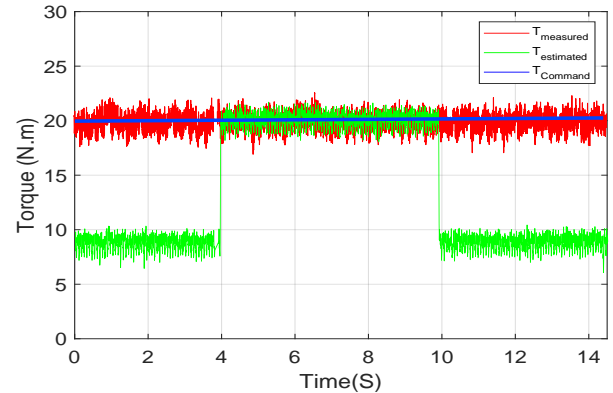


Fig. 8. Torque estimation results without considering g_d, g_q when $t \in [0, 4s]$ and $[10, 14s]$.

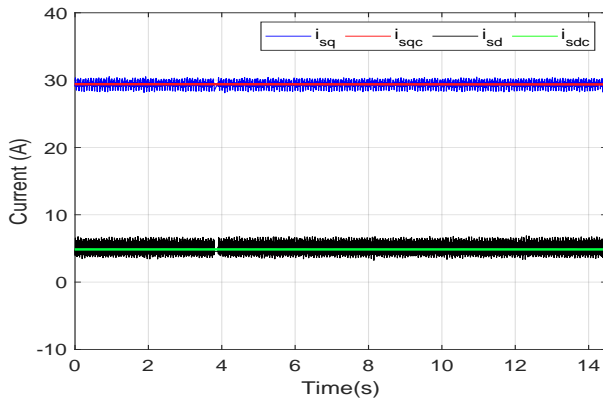


Fig. 9. The currents without considering g_d, g_q .

VII. CONCLUSION

This article proposes a new technique for estimating the torque of wound rotor synchronous machines (WRSM) used in electric vehicles, particularly the Renault ZOE. This technique utilizes a sensorless approach to reduce costs and the congestion, while accounting for magnetic uncertainties and resistance variations. The innovation of this technique, compared to existing methods, lies in the design of a robust LPV state observer, ensuring precise torque estimation in both dynamic and static regimes despite the presence of uncertainties. An observability study of the WRSM and a rigorous proof of the observer's stability and robust performance are provided. Validated through simulations and experimental tests, this technique demonstrates increased efficiency and robustness under real conditions, offering an economical and accurate solution to enhance the safety and control of electric vehicles. These results pave the way for future applications in various types of electric machines used in EVs.

ACKNOWLEDGMENT

This work is supported by the project Chair between Renault Group and Centrale Nantes about performances improvement of electric vehicles propulsion (<https://renault-chair.ec-nantes.fr/>).

REFERENCES

- [1] M. Taherzadeh, M. A. Hamida, M. Ghanes, and M. Koteich, "A new torque observation technique for a PMSM considering unknown magnetic conditions," *IEEE Trans. Ind. Electron.*, vol. 68, no. 3, pp. 1961–1971, 2020.
- [2] M. Taherzadeh, M. A. Hamida, M. Ghanes, and A. Maloum, "Torque estimation of permanent magnet synchronous machine using improved voltage model flux estimator," *IET Electr. Power Appl.*, vol. 15, no. 6, pp. 742–753, 2021.
- [3] M. Ghanes, M. Hamida, A. Maloum, and M. Taherzadeh, "Method for estimating the electromagnetic torque of a synchronous electric machine," February 9 2023, US Patent App. 17/760,084.
- [4] S. Patil, R. Saxena, and Y. Pahariya, "Simulation performance of brushless DC Motor drive using sensorless back EMF detection technique," in *International Conference on Futuristic Technologies (INCOFT)*. IEEE, 2022, pp. 1–4.

- [5] V. S. Virkar and S. S. Karvekar, "Luenberger observer based sensorless speed control of induction motor with fuzzy tuned PID controller," in *International Conference on Communication and Electronics Systems (ICCES)*. IEEE, 2019, pp. 503–508.
- [6] M. Ghanes, M. Hamida, A. Maloum, and M. Taherzadeh, "Method for estimating the electromagnetic torque of a wound-rotor synchronous machine," 2023, wO2023062161 (A1), EPO.
- [7] C. Hoffmann and H. Werner, "A survey of linear parameter-varying control applications validated by experiments or high-fidelity simulations," *IEEE Trans. Control Systems Technology*, vol. 23, no. 2, pp. 416–433, 2014.
- [8] A. Hanif, A. I. Bhatti, and Q. Ahmed, "Managing thermally derated torque of an electrified powertrain through LPV control," *IEEE/ASME Trans. on Mechatronics*, vol. 23, no. 1, pp. 364–376, 2017.
- [9] S. N. Ali, M. J. Hossain, D. Wang, K. Lu, P. O. Rasmussen, V. Sharma, and M. Kashif, "Robust sensorless control against thermally degraded speed performance in an IM drive based electric vehicle," *IEEE Trans. on Energy Conversion*, vol. 35, no. 2, pp. 896–907, 2020.
- [10] Y. Lee, S.-H. Lee, and C. C. Chung, "LPV H_∞ control with disturbance estimation for permanent magnet synchronous motors," *IEEE Trans. Ind. Electron.*, vol. 65, no. 1, pp. 488–497, 2017.
- [11] A. Casavola and G. Gagliardi, "Fault detection and isolation of electrical induction motors via LPV fault observers: A case study," *Int. J. Robust & Nonlinear Control*, vol. 25, no. 5, pp. 627–648, 2015.
- [12] H. Zhang, G. Zhang, and J. Wang, " H_∞ observer design for LPV systems with uncertain measurements on scheduling variables: Application to an electric ground vehicle," *IEEE/ASME Trans. on Mechatronics*, vol. 21, no. 3, pp. 1659–1670, 2016.
- [13] R. Kalman and R. Bucy, "New results in linear filtering and prediction theory," *Journal of Basic Engineering*, vol. 83, no. 1, pp. 95–108, 1961.
- [14] P. Gahinet, P. Apkarian, and M. Chilali, "Affine parameter-dependent Lyapunov functions and real parametric uncertainty," *IEEE Trans. Autom. Control*, vol. 41, no. 3, pp. 436–442, 1996.
- [15] O. Wallmark, L. Harnfors, and O. Carlson, "An improved speed and position estimator for salient permanent-magnet synchronous motors," *IEEE Trans. Ind. Electron.*, vol. 52, no. 1, pp. 255–262, 2005.
- [16] A. Messali, M. Ghanes, M. A. Hamida, and M. Koteich, "A resilient adaptive sliding mode observer for sensorless AC salient pole machine drives based on an improved HF injection method," *Control Engineering Practice*, vol. 93, p. 104163, 2019.
- [17] C. Lascu and G.-D. Andreescu, "PLL position and speed observer with integrated current observer for sensorless PMSM drives," *IEEE Trans. Ind. Electron.*, vol. 67, no. 7, pp. 5990–5999, 2020.
- [18] P. Apkarian, P. Gahinet, and G. Becker, "Self-scheduled H_∞ control of linear parameter-varying systems: A design example," *Automatica*, vol. 31, no. 9, pp. 1251–1261, 1995.
- [19] R. Hermann and A. Krener, "Nonlinear controllability and observability," *IEEE Trans. Autom. Control*, vol. 22, no. 5, pp. 728–740, 1977.
- [20] G. Conte, C. H. Moog, and A. M. Perdon, *Algebraic Methods for Nonlinear Control Systems*. Springer Science & Business Media, 2007.
- [21] R. Hirschorn, "Invertibility of multivariable nonlinear control systems," *IEEE Trans. Autom. Control*, vol. 24, no. 6, pp. 855–865, 1979.
- [22] W. Respondek, "Right and left invertibility of nonlinear control systems," in *Nonlinear Controllability and Optimal Control*. Routledge, 2017, pp. 133–176.
- [23] A. Isidori, *Nonlinear Control Systems*, 3rd ed., ser. Communications and Control Engineering Series. Berlin: Springer-Verlag, 1995.
- [24] S. Boyd, L. El Ghaoui, E. Feron, and V. Balakrishnan, *Linear Matrix Inequalities in System and Control Theory*. SIAM, 1994.
- [25] Q. T. Dinh, S. Gumussoy, W. Michiels, and M. Diehl, "Combining convex–concave decompositions and linearization approaches for solving BMIs, with application to static output feedback," *IEEE Trans. Autom. Control*, vol. 57, no. 6, pp. 1377–1390, 2011.
- [26] Y. Wang, R. Rajamani, and A. Zemouche, "A quadratic matrix inequality based PID controller design for LPV systems," *Syst. Control Lett.*, vol. 126, pp. 67–76, 2019.
- [27] P. Apkarian and R. Adams, "Advanced gain-scheduling techniques for uncertain systems," *IEEE Trans. Control Systems Technology*, vol. 6, no. 1, pp. 21–32, 1998.
- [28] M.-H. Do, D. Koenig, and D. Theilliol, "Robust H_∞ proportional-integral observer-based controller for uncertain LPV system," *J. Franklin Inst.*, vol. 357, no. 4, pp. 2099–2130, 2020.